

Chapter 2 A Strong Motion Velocity Meter in a Modern Seismic Network?

2.1 Introduction

Seismometry has seen huge advances in the past 30 years. The dynamic range of typical seismometers has increased from less than 5 orders of magnitude to more than 7, primarily because of the development of force feedback systems (Wielandt and Streckeisen, 1982; Iwan et al, 1985; Wielandt and Steim, 1986). Advances in recording systems have been even more dramatic; current 24-bit digitisers record over 7 orders of magnitude compared to the 3 orders of magnitude achievable by analogue recording devices (Trifunac and Todorovska, 2001a). The past 30 years have also seen the dramatic development of digital data communication, processing and storage, which has prompted the development of a plan for an Advanced National Seismic Plan (Heaton et al, 1989; Benz and Filson, 1998). These new capabilities allow us to devise new strategies to record ground motions. One such strategy, whose advantages are the subject of this Chapter, would be to deploy continuously telemetered strong motion velocity seismometers in place of existing triggered strong motion accelerometers.

The most critical role of strong motion networks is to provide on-scale recordings of potentially damaging motions over a broad frequency band. Because continuous analogue recording is extremely expensive and strong shaking is infrequent, strong motion seismographs were designed to record only during strong ground shaking. Furthermore, because of the limited dynamic range of recording devices, it was most efficient to record ground acceleration, since near-source strong ground motions have relatively flat acceleration spectra in the band from 0.3 to 3.0Hz.

The typical station specifications for a modern digital network are described, using the California Integrated Seismic Network, CISN, as an example. A CISN station con-

sists of two broadband seismometers, typically a high-gain velocity recording device, such as an STS-2 or a CMG-40T, and a strong motion accelerometer, such as an FBA-23, or EpiSensor. These instruments record on a 24-bit digitiser that has continuous, near-real-time telemetry of high sampled data (80-100*sps*) to the CISN centre at Caltech and USGS-Pasadena.

The main thrust of this Chapter is to discuss whether it would be better to deploy a velocity-recording strong motion instrument in place of existing force-balance accelerometers. Using a large suite of real Earth signals, the hypothetical long-period low-gain velocity seismometer (with a clipping level set to $\pm 5\text{m/s}$) is compared to the existing $\pm 2\text{g}$ clipping Kinematics FBA-23 accelerometer.

It is shown that there are significant advantages in the deployment of the proposed instrument over an accelerometer —

- The velocity instrument would have several orders of magnitude greater sensitivity in the period band from 2*s* to several hundred seconds. This would allow the recording of
 - long-period basin response from regional earthquakes as small as M3.0, and
 - teleseismic ground motions from earthquakes as small as M6,

which could potentially lead to dense spatial recording of small amplitude motions that are not recorded by traditional strong motion networks.

- Furthermore, as well as allowing full recovery of ground acceleration, recovery of ground displacement is likely to be more stable from such a long-period low-gain broadband seismometer.

It is anticipated that a strong motion velocity seismometer would essentially be a low-gain version of existing broadband seismometers, such as the Weilandt-Streckeisen STS-2, and thus its cost would likely be similar to other broadband seismometers. Unfortunately, so would its size and weight. Thus the clear advantages would be offset by significantly poorer cost, size and weight than an accelerometer, which makes it somewhat unwieldy for dense building instrumentation.

At this stage it is pertinent to discuss the design of such an instrument. The STS-2 is designed to respond as a simple single degree of freedom oscillator with free period of 120*s*, with differential feedback, and so has output proportional to ground velocity from

120s to high frequencies. In reality, it consists of a mechanical pendulum with free period of 2s. The feedback electronics produce a heavily over-damped ($\sim 1000\%$ of critical) output, and so the suspension displacement is proportional to ground velocity over a wide frequency band about this free period. Chapter 3 presents an investigation into a relatively new Japanese strong motion velocity recording sensor, the VSE-355G2. This instrument has a mechanical pendulum of about 3Hz with a similar feedback system. Unfortunately it is also slightly heavier (20kg), and larger (30cm x 30cm plan x 20cm high) than the STS-2.

A strong motion velocity seismometer could record a broader swath of Earth motions than are currently recorded by existing strong motion accelerometers. With a clipping level of $\pm 5\text{m/s}$ (a velocity magnitude greater than that of any seismic ground motion measured to date) it would recover on-scale all motions relevant to structural engineering, and it would record long-period motions with accelerations too small to be recorded by traditional accelerometers. It is estimated that direct recording of velocity with a dynamic range of 140dB would permit recording of broadband motions from regional and near-source events as small as M3.0. These broadband motions could be used to study path effects such as the amplification of long-period motions by basins. In addition, a strong motion velocity array should be capable of recording teleseisms as small as M6. This could lead to dense spatial recording of small amplitude motions that are not recorded by traditional strong motion networks.

Single differentiation of the raw velocity output would produce the acceleration records currently used by engineers. However, the real issue is not acceleration versus velocity, but is one of having accurate motion in the frequency band of interest. The velocity seismometer has the significant advantage that displacement estimates of ground motion would be obtained from a single integration of the raw data. Current strong motion velocity devices have flat responses up to 70Hz, so acceleration timeseries can be recovered up to this frequency, which is satisfactory for most engineering purposes, as few structures are damaged by energy at 70Hz. Further, as long as the longest frequencies in a signal are below the low frequency corner of the instrument ($\sim 100\text{s}$ — in effect excluding all but static offsets), single integration would result in smaller long period error than would a double integration, assuming a similar error in the true signal of velocity and acceleration. Single integration

thus leads to a more stable and conclusive set of displacement time series, especially with regard to static offsets. Even very small baselines or linear trends, which are difficult to isolate and remove in current strong motion records, can seriously distort the resultant displacement after double integration, often leaving its estimation more a matter of judgment rather than science (Boore, 2001). Resolving long-period motions associated with static displacements is somewhat more complicated, as will be discussed in Chapters 3 and 4. Essentially, as the instrument response of the strong motion sensor needs to be removed to recover the zero frequency static offset, the strong motion velocity meter provides no improvements over traditional accelerometers for this. As the velocity meter is also an inertial seismometer like the accelerometer, the sensor is also very sensitive to tilt. Small changes in tilt can significantly affect the derivation of ground displacement, as pointed out by Trifunac and Todorovska (2001b). In order to fully derive the translational displacements in the presence of tilt requires additional information from a co-located rotational meter, or a nearby true displacement meter, such as GPS.

The increased range of Earth recordings obtained from using the proposed strong motion velocity seismometer is demonstrated through comparisons of signal recovery with both a typical accelerometer, the Kinemetrics FBA-23, and a broadband velocity instrument, the Weilandt-Streckeisen STS-2. The performance of each device is illustrated by showing how their dynamic characteristics relate to a wide range of seismic motions, in terms of frequency content and acceleration amplitude. An in-depth description of the components of the complete seismographic system — which includes a digital recording device as well as the seismometer — and how the dynamic range is finally determined, is first presented.

2.2 A Typical CISN Station

The California Integrated Seismic Network (CISN), www.cisn.org, is the network source of most of the data used not only in this Chapter, but throughout the thesis. The CISN collates data from the Southern California Seismic Network (SCSN), the Northern California Seismic Network (NCSN), and many strong motion networks around the State of Califor-

nia. Data is available from the individual network data centre Web portals: the Southern California Earthquake Data Center (SCEDC), www.scecdc.scec.org, the Northern California Earthquake Data Center (NCEDC), quake.geo.berkeley.edu, and the Consortium of Organizations for Strong Motion Observation Systems (COSMOS) Strong Motion Virtual Data Center, www.cosmos-eq.org. CISEN is a recent amalgamation of the three existing organisations. Most data herein is from the SCSN. This network has immensely benefited from the TriNet project (1997-2001). TriNet provided a dense, modern seismic information system for Southern California (Hauksson et al, 2001; Hauksson et al, 2003), with over 150 broadband stations. TriNet itself grew out of the first digital, co-ordinated broadband and strong motion seismic network in Southern California, TERRAScope (Kanamori et al, 1991), which comprised 28 stations.

The SCSN is designed to record on-scale motions from an M8 earthquake, as well as large teleseismic earthquakes and small regional motions. The entire network has a minimum earthquake detectability threshold of M1.8. This requires not only an even and relatively dense distribution of stations, but each station must also have a very large dynamic range, of about 10 orders of magnitude, or $200dB$. Thus the typical station consists of two broadband force-balance seismometers, typically a high-gain velocity recording device, such as an STS-2 or a CMG-40T, and a low-gain strong motion accelerometer, such as an FBA-23, or EpiSensor. These instruments record on a 24-bit Quanterra digitiser — about 7 orders of magnitude dynamic range, or $138dB$. A plot of the dynamic range of the typical sensor/datalogger configuration is in Figure 2.1, which also includes the average size of earthquake signals from events of various magnitudes and distances. A detailed explanation of how this plot was produced is in Sections 2.4 and 2.5. The digitiser has continuous, near-real time telemetry of high sampled data ($80 - 100sps$) to the data processing and archiving centres at the Caltech Seismological Lab, located in the South Mudd Laboratory at Caltech, and across the road from South Mudd, at the USGS Pasadena office, 525 S. Wilson Ave. The digitisers can also log the continuous (in a 3-week buffer) and triggered data locally in the event of a transmission breakdown.

The data processing centres receive continuous data from more than 1200 high sample channels ($100sps$, $80sps$), and over 2000 lower sample channels ($20sps$, $1sps$, $0.1sps$,

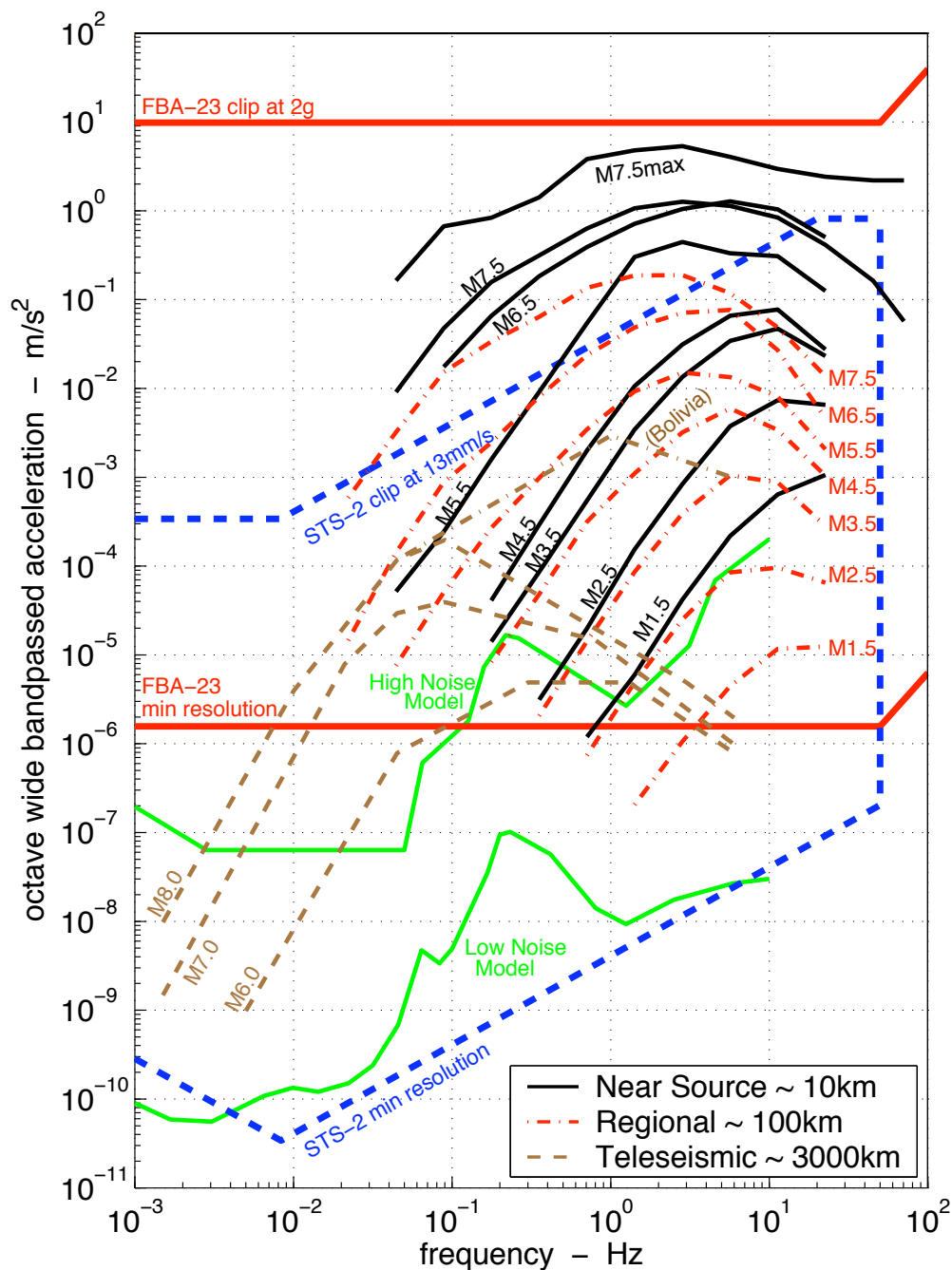


Figure 2.1: Frequency - amplitude plot for octave wide bandpasses of ground motion acceleration. A typical CISON station records all motions located between the FBA-23 clip and the STS-2 minimum resolution, encompassing the ~ 10 orders of magnitude required to cover the Earth's signals. Assumes 24-bit digitiser. Note that instrument limits are scaled down to account for the bandpassing of the event data. Ground motions recorded on-scale by the FBA-23 lie between the thick solid lines. The thick dashed lines give the dynamic range of the STS-2. Noise levels are the USGS High and Low Noise Models (Peterson, 1993).

health monitoring channels).

In certain cases, especially for stations in noisy areas, such as buildings, only a strong motion accelerometer is deployed with the 24-bit digitiser. This is the case at many of the stations around Caltech Campus, such as the Millikan Library (MIK), the Broad Center (CBC) and the USGS Building (GSA). Some other stations, such as the Caltech Athenaeum (CAC), have only an accelerometer alongside a 19-bit K-2 digitiser.

Other remote stations may only have a short period Mark Products L4-C vertical instrument with limited dynamic range of about $55dB$, primarily used for earthquake detection and location.

In total the SCSN currently has about 155 stations with both broadband and strong motion sensors, with about 55 stations with a single 3-component strong motion sensor. There are also about 140 stations with vertical component short period sensors only. A station location map for the entire SCSN is in Figure 2.2, and Figure 2.3 is a close up of the LA basin.

The data is stored in both a continuous format, at $20sps$, and in triggered ‘event’ format, at $80-100sps$, at the Southern California Earthquake Data Center, SCEDC. The digitisers are all Quanterra models, the older dataloggers have a maximum sampling rate of $80sps$, the new models $100sps$. Triggered event data is available a few hours after an event is identified, and continuous data for the previous day is made available at 12AM GMT.

Summary tables of typical instruments and digitisers are in Tables 2.1 and 2.2. The instrument response for the broadband sensors is in Figure 2.4. The broadband instrument response is flat to velocity for all the instruments from about $7Hz$ (the other instruments have their high frequency cutoff all beyond $20Hz$) to $30s$ and further, up to $360s$. Beyond the long-period period corner, all sensors have a drop-off at a rate of $-12dB/oct$ to velocity, which means in this recording range, the instruments are flat to the differential of acceleration (the ‘jerk’). At frequencies less than the high frequency cutoff, these instruments all respond essentially as single degree of freedom (SDOF) simple oscillators with differential feedback.

Data is available via a Web browser at www.scecdc.scec.org/stp.html, or from a stand-alone software version on the users computer, downloadable from www.scecdc.

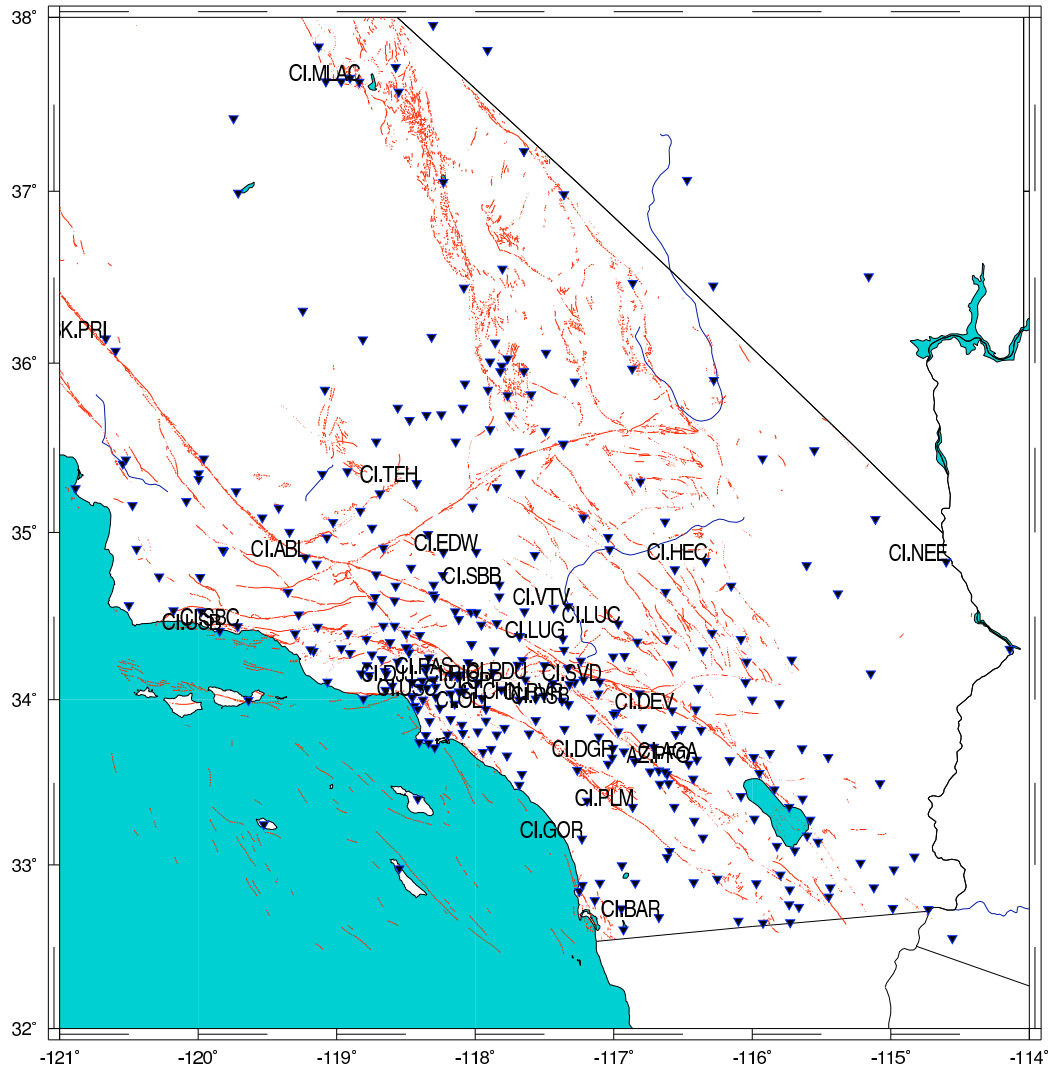


Figure 2.2: Southern California Seismic Network (SCSN) station map. Known faults are in light shade. A selection of station names is shown.

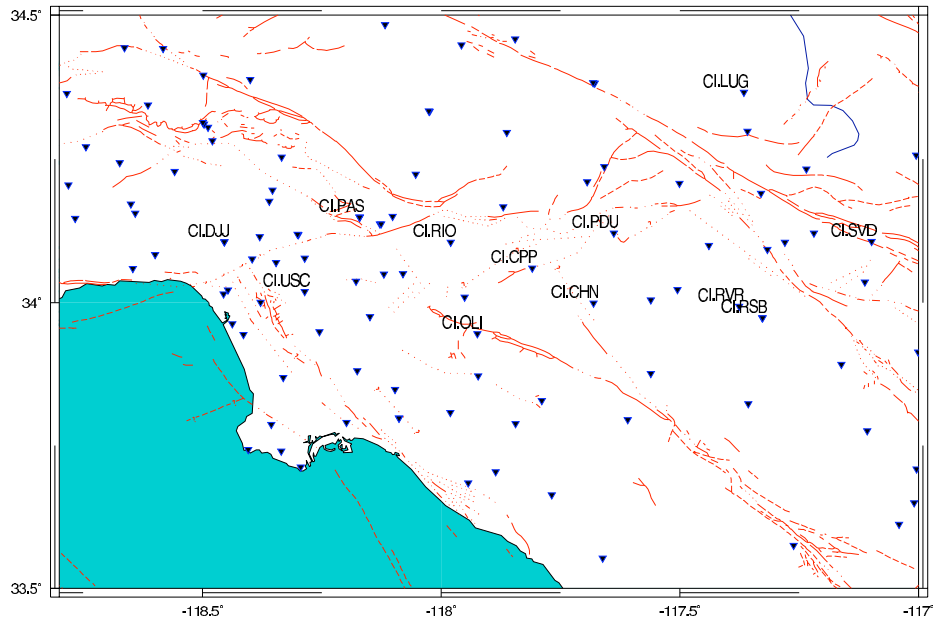
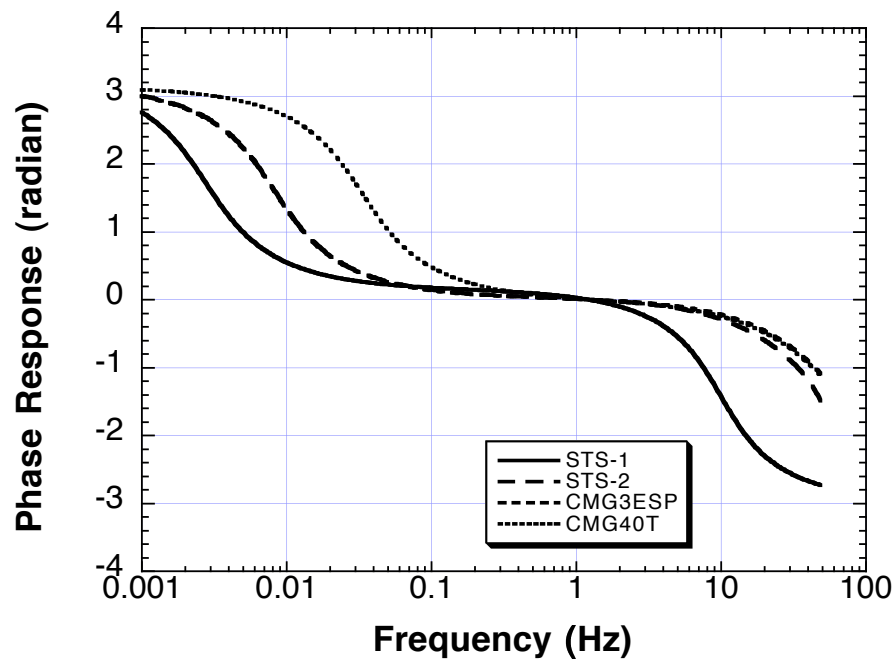


Figure 2.3: Southern California Seismic Network (SCSN) station map for the Los Angeles basin. Known faults are in light shade. CI.PAS is station at Kresge Lab., Pasadena.

| Manufacturer | Type | Freq. Range | Sensitivity | Clip Level |
|---|-----------|-------------|--------------------|------------|
| <i>High Gain Broad-Band Seismometers :</i> | | | | |
| Streckeisen | STS-1 | 0.0027-10Hz | 2500 V/m/s (vert) | ~ 0.8cm/s |
| | | | 2300 V/m/s (horiz) | ~ 0.8cm/s |
| Streckeisen | STS-2 | 0.0083-50Hz | 1500 V/m/s | 1.3cm/s |
| Guralp | CMG-1T | 0.0027-10Hz | 1500 V/m/s | ~ 1cm/s |
| Guralp | CMG-40T | 0.033-50Hz | 800 V/m/s | ~ 1cm/s |
| Guralp | CMG-3ESP | 0.0083-50Hz | 2000 V/m/s | ~ 1cm/s |
| Guralp | CMG-3T | 0.0083-50Hz | 1500 V/m/s | ~ 1cm/s |
| <i>Low Gain Broad-Band (Accelerometer/Strong Motion Velocity) :</i> | | | | |
| Kinometrics | FBA-23 | DC-50Hz | 5 V/g | 2g |
| Kinometrics | EpiSensor | DC-180Hz | 10 V/g | 2g |
| Tokyo-Sokushin | VSE-355G3 | ~.01-70Hz | 10 V/m/s | ~ 200cm/s |

Table 2.1: Summary of typical instruments used in the California Integrated Seismic Network. Abridged from Hauksson et al. (2001)

(a)



(b)

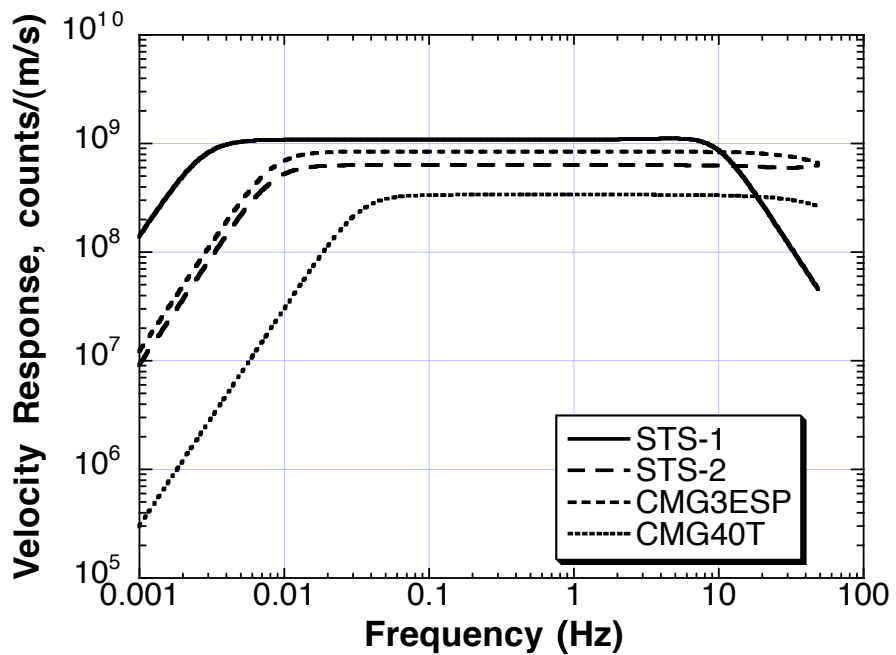


Figure 2.4: Response for typical broadband CISN instruments (from Hauksson et al. (2001)).

| Manufacturer | Type | Site Recording | Channels | Max. SPS | Volts/cts |
|--------------|-------|----------------|----------|----------|--------------|
| Quanterra | Q980 | 1.6Gb | 9 | 80 | $20/2^{23}$ |
| Quanterra | Q380 | 1.6Gb | 3 | 80 | $20/2^{23}$ |
| Quanterra | Q680 | 1.6Gb | 6 | 80 | $20/2^{23}$ |
| Quanterra | Q4128 | 1.6Gb | 8 | 100 | $20/2^{23}$ |
| Quanterra | Q730 | 1.6Gb | 6 | 100 | $16/2^{23}$ |
| Quanterra | Q730E | 280Mb | 6 | 100 | $16/2^{23}$ |
| Quanterra | Q330 | 20Gb | 6 | 200 | $20/2^{23}$ |
| Kinematics | K2 | 64Mb | 4 | 100 | $2.5/2^{23}$ |

Table 2.2: Summary of typical digitisers used in the California Integrated Seismic Network. Abridged from Hauksson et al. (2001)

scec.org/ftp/programs/stp. This later version can be opened using perl scripts for automated searching and downloading of data.

2.3 The Definition of Dynamic Range

Following Heaton (2003), the dynamic range, DR , of an instrument is defined as the ratio of the largest on-scale/linear measurement, M_{max} divided by the smallest measurement resolvable by the instrument, M_{min} :

$$DR = \frac{M_{max}}{M_{min}} \quad (2.1)$$

In the context of seismic instrumentation, the measurement is usually voltage output for a seismometer, or counts for a digitiser.

Traditionally, dynamic range is given in the units of decibels (dB), $\frac{1}{10}^{\text{th}}$ of a Bel. A Bel is defined as a base 10 logarithmic measure of energy per unit time, or power. Since the power of a signal is proportional to the square of the signal amplitude:

$$DR_{dB} = 10 \log_{10} \left[\frac{M_{max}}{M_{min}} \right]^2 dB \quad (2.2)$$

$$= 20 \log_{10} \left[\frac{M_{max}}{M_{min}} \right] dB \quad (2.3)$$

The Earth, for example, has about 10 orders of magnitude range in intensity from the largest motions from large earthquakes to the noise levels at the quietest sites (such as recorded at depth in a mine shaft in a seismically inactive region far from the ocean). Thus the dynamic range of the Earth is:

$$DR_{dB}(Earth) = 20 \log_{10} \left[\frac{10^{10}}{1} \right] dB \quad (2.4)$$

$$= 200dB \quad (2.5)$$

Similarly, m orders of magnitude dynamic range is equivalent to $(20 * m)dB$.

Seismic recordings made on traditional recording paper have a maximum amplitude of about $10cm$, and a minimum resolution of about $0.1mm$. This is a dynamic range of 3 orders of magnitude, or $60dB$.

Modern seismometers record on digital recorders, which convert the analogue voltage seismometer output to digital counts. The nominal dynamic range is determined by the number of bits used to characterise the voltage. One bit is used to determine whether the signal is positive or negative, and each additional bit represents a factor of 2 in dynamic range, so dynamic range is 2^{n-1} . For a 24-bit digitiser, the dynamic range is 2^{23} or 8388608. This is $138.5dB$, or $138.5dB/20 \sim 7$ orders of magnitude.

[An alternative, quick way to determine the dynamic range of a digitiser in dB is $DR_{dB} = (\#bits - 1) * 6.02$, as each additional bit increases the dynamic range by $20 \log(2) = 6.02$.]

2.4 The Seismographic System

The range of amplitude and frequency recorded by a modern seismographic system is controlled by both the seismometer and the digitiser, or digital recorder. Ideally, the maximum gain of the datalogger ($2^{(n-1)}$ counts for a n -bit system) should be reached when the instrument is at its clip level. If so, the minimum resolution of the seismographic system is determined by lowest resolution of the instrument and digitiser. Thus, the dynamic range

of the 2 components is investigated separately, to fully understand the dynamic range of the complete system.

Similarly, the behaviour of a system at clipping is dependent on the clipping characteristics of both the datalogger and sensor. With regards to the datalogger, many n -bit instruments simply cannot measure/output any more than 2^{n-1} counts, and will flat-line if the input signal is larger than this. Modern Quanterra 330 series instruments are in fact 27-bit sensors, though linearity of signal output is only guaranteed up to 24-bit. Thus the output can measure above 2^{23} or 8,388,608 counts. Similarly, the instruments manufacturers design the instruments only to guarantee linearity up to the advertised clip level. Once this has been exceeded, a range of signal errors can occur, ranging from the relatively innocuous (and this very difficult to recognise as incorrect) small drift away from linearity, to spikes, flat-lines and long-period instrument responses. Many of these will be observed in practice in the subsequent Chapters.

2.4.1 Dynamic Range of the Digital Recorder

Current state-of-the-art digital recorders employ 24-bit digitisers. The nominal dynamic range of such a device is about $140dB$. Theoretically, the dynamic range can exceed $140dB$ at low frequencies, since low frequency signals are oversampled and each point is the average of many samples. However, this dynamic range enhancement does not occur where the noise is characterised by a power density that increases as frequency decreases, i.e., some form of $1/f$ noise. This type of noise has a constant power in frequency bands of equal relative width (Wielandt and Streckeisen, 1982). Most electronic systems, in fact, are characterized by $1/f$ noise below 1Hz, and hence no resolution enhancement occurs (Joe Steim, personal communication, 2001). In practice, under normal operating temperatures, the dynamic range can indeed increase. For example, the Quanterra Q330, with $135dB$ nominal dynamic range, at $26^{\circ}C$ records $136dB$ at $10Hz$, up to $142dB$ at $0.5Hz$, before dropping slightly at lower frequencies (Joe Steim, personal communication, 2001). As this is not a very large difference, I will assume, for the purposes of this work, a frequency-independent constant dynamic range of $140dB$, approximately 7 orders of magnitude, for

the digitiser.

2.4.2 Dynamic Range of Each Seismometer

– FBA-23

The clipping limit of the FBA-23 seismometer is $\pm 19.6m/s^2$ ($\pm 2g$) up to its corner frequency of $50Hz$. By comparing ground motions recorded simultaneously with the FBA-23 and STS-2, it was established that the FBA-23 can resolve acceleration above the noise level of the instrument down to about $3 \times 10^{-6}m/s^2$ across a broad band of frequencies (0.01 to $10Hz$). This is illustrated in Figures 2.13 and 2.14, from Section 2.5, which show the bandpassed records of a M8.1 event at $2900km$ epicentral distance. The FBA-23 noise at periods of about $100s$ and $50s$ are both of this level. For example, in Figure 2.14, the noise level is approximated as a sine wave with a $100s$ period and amplitude $5 \times 10^{-5}m/s$:

$$\begin{aligned} \dot{u}_{noise} &= 5 \times 10^{-5} \sin 2\pi f \tau \quad m/s \\ &= 5 \times 10^{-5} \sin(6.28 \times 10^{-2}) \tau \quad m/s \\ \Rightarrow \ddot{u}_{noise} &= 3.14 \times 10^{-6} \cos(6.28 \times 10^{-2}) \tau \quad m/s^2 \end{aligned}$$

and thus the amplitude of this wave in acceleration is approximately $3.14 \times 10^{-6}m/s^2$, $136dB$ below the clip level of $\pm 19.8m/s^2$. This is less than the published $145dB$ for the frequency range 0.01 to $20Hz$ (www.kinematics.com), but could also be due to limitations of the digitiser.

Further evidence for this noise level can be seen in Figure 2.5. In this plot, real continuous ambient noise data from a selection of accelerometer/digitiser configurations in the SCSN is presented. On average, FBA channels record noise at about $136dB$ below the clip level, whilst the EpiSensor has a better dynamic range, nearer $140dB$. This general trend, with a relatively constant amplitude over a wide band-width, occurs for a variety of stations and digitisers, which indicates this observed noise line is the actual noise floor of the instrument, rather than station's local site noise, or digitiser noise.

For the purposes of this work, it is thus assumed the dynamic range of the FBA ac-

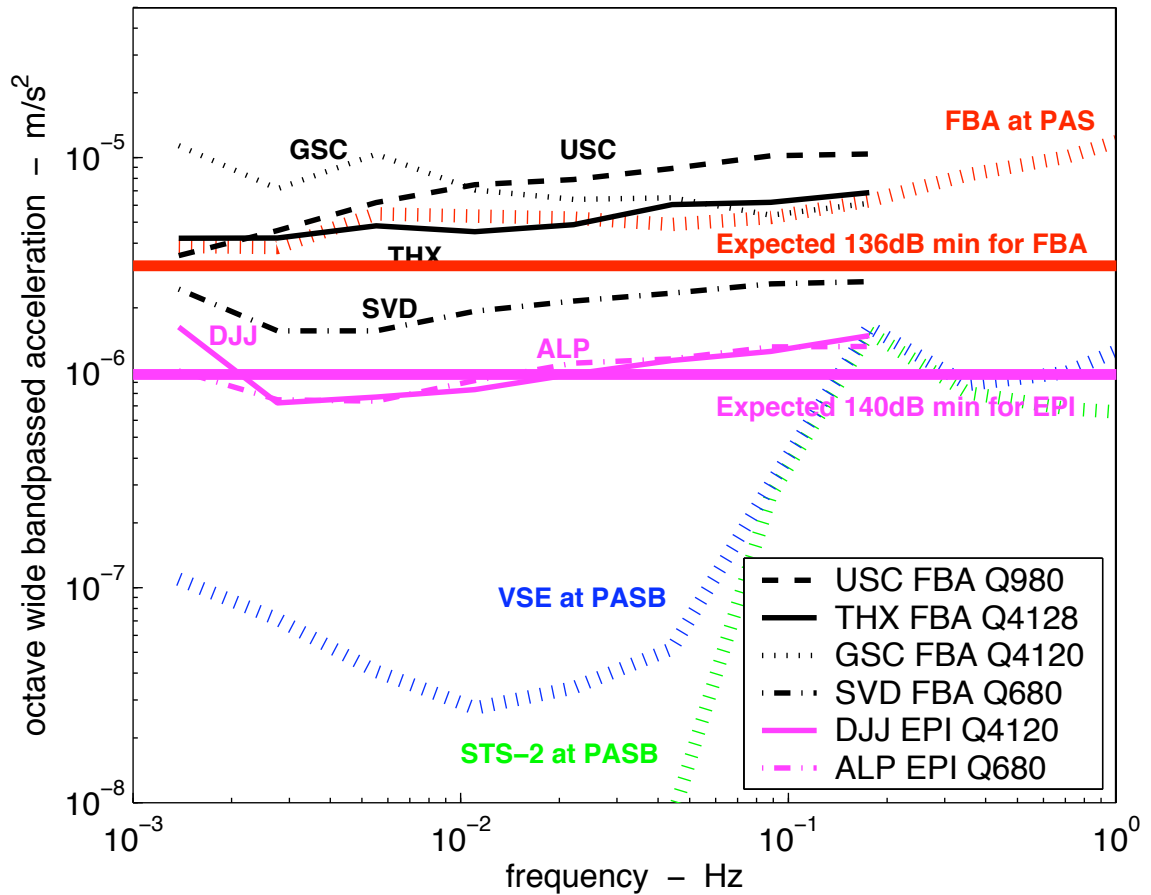


Figure 2.5: Comparison of noise floors for various accelerometer/digitiser configurations deployed in SCSN. All station data from a 3hour period on 1 April 2002. Also includes data from test station PASB, which at the time of the comparison, housed a Japanese Strong Motion Velocity Meter, the VSE-355G2, and an STS-2. PAS and PASB are essentially co-located.

celerometer is $136dB$ for the frequency range from $50Hz$ - DC.

– STS-2

Broadband seismometers such as the STS-2 have more complex characteristics. For seismic signals with periods shorter than the corner frequency ($120s$ for an STS-2), they typically have clip levels that are given in both velocity and acceleration; in the case of the STS-2 this is $\pm 13mm/s$ and $\pm 3.3m/s^2$ ($\pm 0.34g$). Velocity clip levels are often given as peak-to-peak values, for the STS-2 this would be $26mm/s$ peak-to-peak, hence the $1/2$ peak-to-peak value is $13mm/s$. The minimum resolvable motion for the STS-2 is not a simple function, or indeed directly related to the clip; in fact it is highly dependent on frequency, and is greater than $140dB$ for the frequency range of interest. The instrument noise level is published in the STS-2 manual (Streckeisen and Messgerate), and is shown in Figure 2.6.

– Strong Motion Velocity Meter

The hypothetical long-period, low-gain velocity instrument would have a similar type of response as the STS-2, with a corner frequency at $120s$, and clip level at $\pm 5m/s$ and $\pm 49m/s^2$ ($\pm 5g$). Minimum resolution is assumed to be $140dB$ below the clip level, a similar value to both the STS-2 and FBA-23.

The dynamic characteristics of these three seismometers are summarised in Table 2.3, and illustrated in Figure 2.6.

| Instrument Type | Free Period | Clip Level |
|------------------------|-----------------------|--|
| FBA-23 | $0.02s$ ($50Hz$) | $\pm 19.6m/s^2$ ($\pm 2g$) |
| STS-2 | $120s$ ($0.0083Hz$) | $\min[\pm 13mm/s, \pm 3.3m/s^2$ ($\pm 0.34g$)] |
| strong motion velocity | $120s$ ($0.0083Hz$) | $\min[\pm 5m/s, \pm 49m/s^2$ ($\pm 5g$)] |

Table 2.3: Comparison of important properties of the instruments

The final response of the seismographic system is similar to the instrument response, but the system dynamic range at any frequency does not exceed $140dB$ due to the limitations

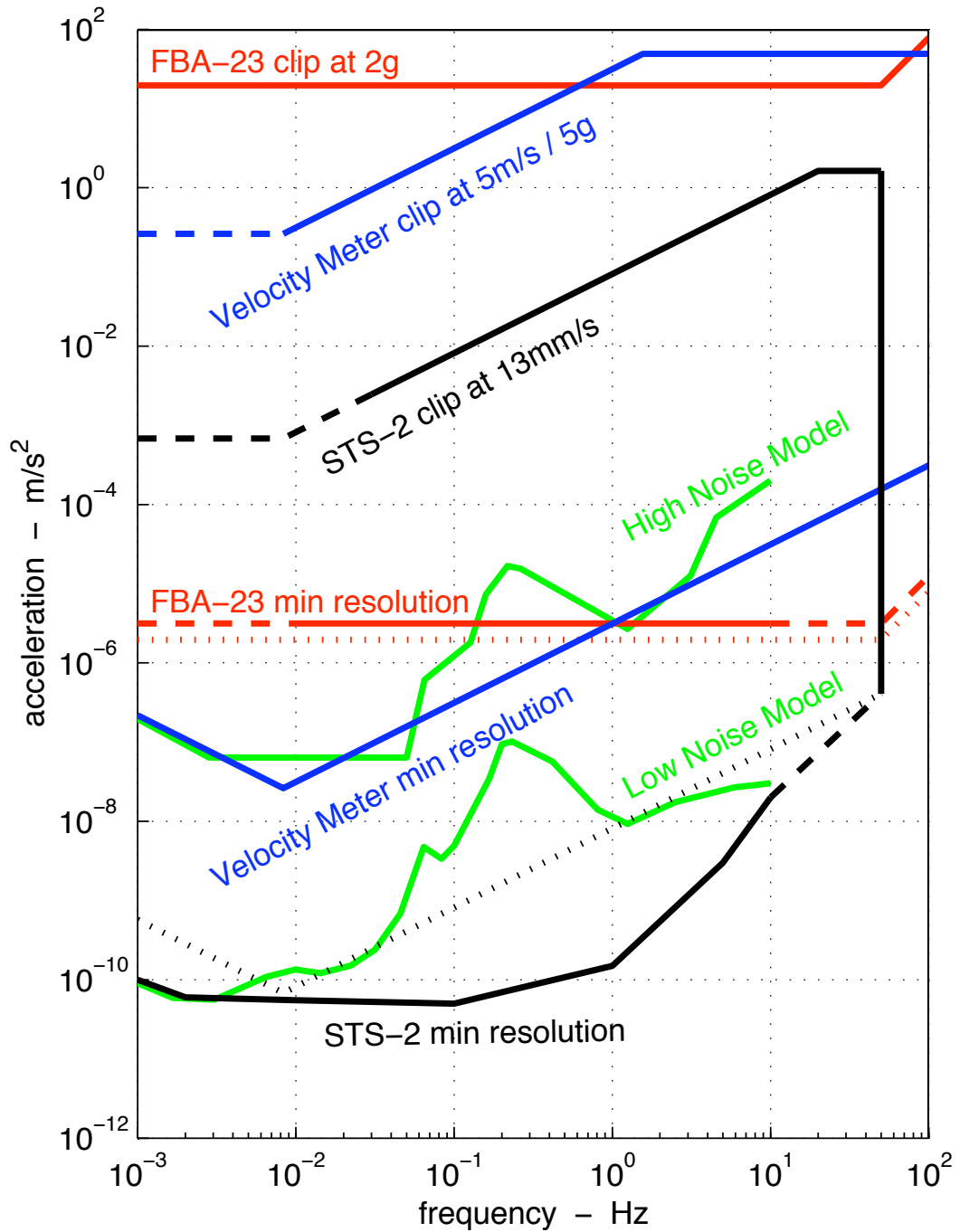


Figure 2.6: Instrument responses in terms of acceleration. Dashed lines indicate regions of uncertain instrument response. For the FBA-23 and STS-2, dotted lines indicate areas 140dB below instrument clipping levels. Noise levels are the USGS High and Low Noise Models (Peterson, 1993).

of the digitiser. For the three instruments, only the system response for the STS-2 system is affected.

Note that for brevity and simplicity, hereafter the combined seismographic system comprising both the instrument and digitiser is referred to simply as the ‘instrument’ or the ‘seismometer’.

2.5 Strong Motion Instrument Comparisons Using Recorded Earthquake Signals

The hypothetical strong motion velocity meter is compared with the Kinematics FBA-23 accelerometer, and the Weilandt-Streckeisen STS-2 broadband velocity seismometer. To show the range of motions typically recorded on-scale and above the instrument noise of each instrument, their performance in frequency and amplitude of acceleration is plotted in relation to a broad range of Earth signals typically of interest to engineers and seismologists. Measured signal strengths of each record are not power spectra of the broadband time series, but discrete octave-wide bandpasses. This allows the inconsistencies in the power spectra associated with arbitrarily picking a duration for the transient earthquake signals (Aki and Richards, 1980) to be ignored. Although this also means the complexity of the overall broadband signal is ignored (and will then in general under-represent the final strength of the record), bandpassing facilitates a better relation of the instrument limits to signal strength.

2.5.1 Assembly of the Earthquake Database

The earthquake signals selected were divided into magnitude-distance bins, summarised in Table 2.4. For each distance, the bins vary in increments of one magnitude unit, for example, the M6.5 bin incorporates data from M6.0 to M6.9 events. The three distance bins represent near-source, regional and teleseismic recordings.

The records in the near-source database were generally limited to data from within *10km* distance from the projection of rupture onto the Earth’s surface. Event magnitudes

| 1. NEAR SOURCE : data within 0 – 20km of epicenter (or surface projection of rupture) | | | | |
|--|------------------|-----------------|-----------------|----------------------------------|
| Magnitude | #stations | #records | events | instruments — data source |
| M7.5 | 26 | 78 | Chi-Chi '99 | A800,A900 Geotech — CWB Taiwan |
| | 5 | 14 | Koaceli '99 | SMA-1(5xGSR-16) — ERD,Kandilli |
| M6.5 | 9 | 26 | Northridge '94 | SMA-1 (3xFBA-23) — UCSB |
| | 14 | 41 | Imp. Valley '79 | SMA-1 (3xDCA-10) — UCSB |
| | 1 | 3 | Coalinga '83 | SMA-1 — UCSB |
| M5.5 | 3 | 8 | 3 | 8 x FBA-23 — TriNet |
| M4.5 | 28 | 84 | 20 | 32 x FBA-23, 52 x STS-2 — TriNet |
| M3.5 | 10 | 62 | 21 | 32 x FBA-23, 30 x STS-2 — TriNet |
| M2.5 | 12 | 108 | 35 | 108 x STS-2 — TriNet |
| M1.5 | 8 | 42 | 12 | 42 x STS-2 — TriNet |

| 2. REGIONAL : data within 90 – 110km of epicenter (or surface projection of rupture) | | | | |
|---|------------------|-----------------|---------------|----------------------------------|
| Magnitude | #stations | #records | events | instruments — data source |
| M7.5 | 16 | 48 | Chi-Chi '99 | A800,A900 Geotech — CWB Taiwan |
| | 2 | 6 | Koaceli '99 | 6 x GSR-16 — ERD Turkey |
| M6.5 | 4 | 12 | 2 | 12 x STS-2 — TriNet |
| M5.5 | 11 | 51 | 7 | 24 x FBA-23, 27 x STS-2 — TriNet |
| M4.5 | 13 | 52 | 5 | 10 x FBA-23, 42 x STS-2 — TriNet |
| M3.5 | 13 | 96 | 23 | 96 x STS-2 — TriNet |
| M2.5 | 12 | 66 | 20 | 66 x STS-2 — TriNet |
| M1.5 | 10 | 39 | 12 | 39 x STS-2 — TriNet |

| 3. TELESEISMIC : data about 3000km (27°) from epicenter, records usually 20sps (or equivalent), up to 1 hour duration) | | | | |
|---|------------------|-----------------|---------------|----------------------------------|
| Magnitude | #stations | #records | events | instruments — data source |
| M8 | 19 | 57 | 9 | STS-1,2, KS5400,3600 — IRIS GSN |
| M7 | 20 | 60 | 7 | STS-1,2, KS5400,3600 — IRIS GSN |
| M6 | 13 | 39 | 8 | STS-1,2, KS5400,3600 — IRIS GSN |

Table 2.4: Summary of waveform data included in each Magnitude-Distance bin. For the teleseismic datasets — M8 is represented by events in the range M7.6 - M8.0, at 21° - 31° and 33 - 480km depth, with 2 additional records from the M8.2 637km deep focus Bolivia event at 20° — M7 is represented by events in the range M6.8 - M7.4 at 23° - 29° and 10 - 185km depth — M6 is represented by events all of M6 at 25° - 29° and 10 - 49km depth.

range from M7.5 down to M1.5. Records were obtained from the SCEDC database (then TriNet) (www.trinet.org; www.scecdc.scec.org/stp.html) (Hauksson et al, 2001). Due to a sparsity of data from events of M6 and above, the distance limit was relaxed to include records under 20km from the projection of rupture. For these larger events, data is also included from the Southern California Earthquake Center (SCEC) Strong Motion Data Base (SMDB) (now part of COSMOS, <http://db.cosmos-eq.org/>) for historic events, with records from predominantly analogue instruments, and from Taiwanese (Lee et al, 1999; Uzarski and Arnold, 2001) and Turkish (www.koeri.boun.edu.tr; www.deprem.gov.tr; Youd et al, 2000) data centers for timeseries from recent large earthquakes outside of Southern California.

The regional database was represented by records at a distance of about 100km . Event magnitudes range from M7.5 down to M1.5. As with the near-source database, the distance bin was relaxed to include records within $85 - 110\text{km}$ of the projection of rupture onto the Earth's surface for the sparse data sets from the larger magnitude events. The data sources were the same as those for the near-source database.

Records in the teleseismic database were limited to signals recorded at about 3000km epicentral distance. Data from M8 to M6 events were used, obtained from the IRIS-GSN Web site (www.iris.washington.edu).

Each bin contained records from a wide sampling of events and stations in order to obtain reasonable median values of peak amplitude. The only event which contained data which seriously deviated from the median was the M8.2 deep focus Bolivia event, which is treated separately.

All timeseries from broadband velocity instruments were differentiated to acceleration.

2.5.2 Recovery of Earth Signals

Once the database was assembled, each individual timeseries was passed through octave-wide bandpass filters. The absolute maxima of each bandpass for each record was recorded, as illustrated for 2 very different signals in Figure 2.7 and Figure 2.8. The maximum frequency for the bandpasses for each magnitude-distance bin was determined by the Nyquist

value of the timeseries. The minimum frequency was more subjectively chosen as the frequency where the signal intensity was similar to the background noise.

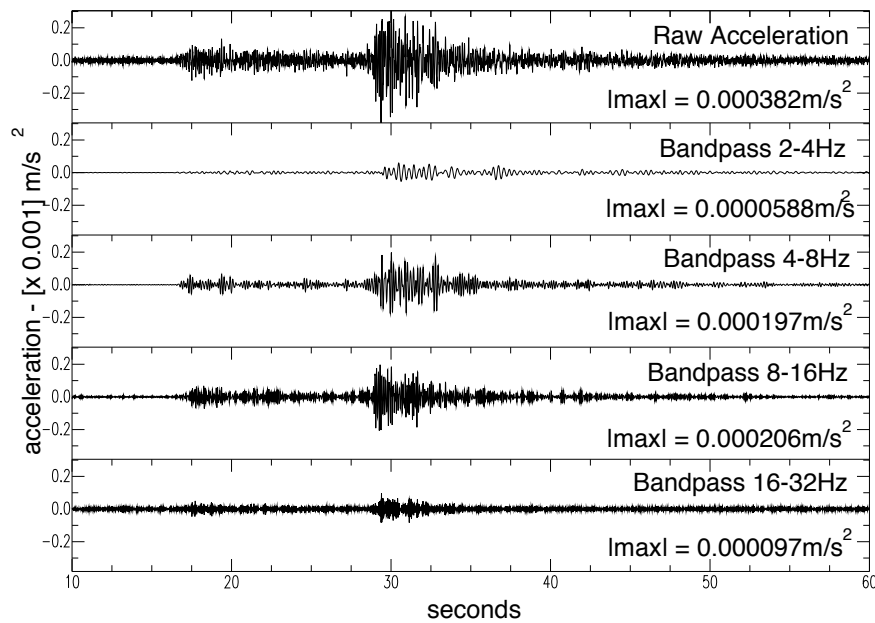


Figure 2.7: Sample bandpasses for M3.5 at 100km (acceleration records from 3 February 1998 event, recorded at Station LKL on the 80sps N-S component channel of an STS-2.

For each bandpass of a magnitude-distance bin, the geometric mean of all the absolute maxima was calculated. When combined with the geometric means from the other bandpasses in the same bin, a curve is obtained which represents the octave-wide frequency content typical of ground motions for that bin. This is demonstrated for the M3.5 at 100km magnitude-distance bin in Figure 2.9.

The frequency-amplitude curves for all the magnitude-distance bins are shown in Figure 2.1. In this Figure, also shown are the dynamic range performances of the instruments typically installed at a CISN station. Figure 2.10 includes the hypothetical low-gain velocity meter.

The limits of the individual instruments to the broadband signals have been discussed (see Figure 2.6). The ground motion data plotted has been bandpass filtered, and to account for this, there is a need to modify, or calibrate, the broadband instrument clip levels for an octave-wide clip level. To do this, first a number of broadband timeseries are chosen which are close to clipping each instrument (generally within 20% of saturation). These records

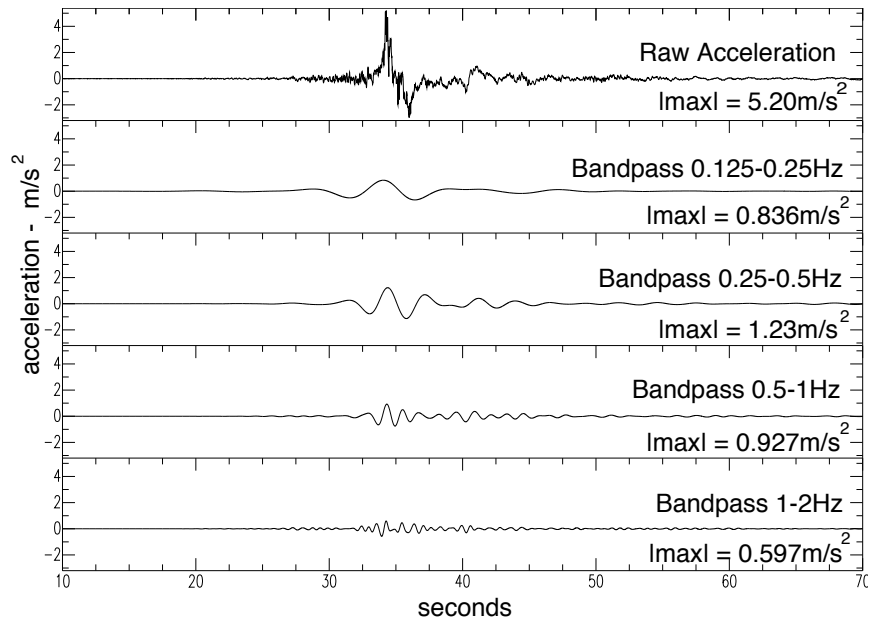


Figure 2.8: Sample bandpasses for M7.5 at 10km (acceleration records from 21 September 1999 Chi-Chi earthquake, recorded at Station T076 on the 200sps Z component channel of a Geotech A900).

are then filtered in octave-wide bandpasses. To calibrate the instruments, the bandpass with the highest velocity (for the broadband STS-2 seismometer) or acceleration (for the FBA-23) is selected, this maximum value is scaled by the reciprocal of the percentage the timeseries came to the clip level for the instrument. This new value is the calibrated clip level for the bandpassed data. The inherent uncertainty in this method was reduced by performing this for a number of records of varying spectral content. Typically this reduced the broadband clipping levels by about 50% .

Finally, the New High and Low Noise Models from Peterson (1993) were superimposed onto Figures 2.1 and 2.10.

The ‘M7.5Max’ line on Figures 2.1 and 2.10 was derived from some of the largest near-source waveforms ever recorded, including data from the recent Chi-Chi, Taiwan, and Kocaeli, Turkey events. The line is constructed using the absolute maxima of each bandpass for the M7.5 at 10km dataset (not the geometric mean). From all these records, it is clear that both the $\pm 19.6 \text{ m/s}^2$ FBA-23 and hypothetical low-gain velocity instrument are unlikely to clip in the event of most conceivable Earth motions. In this regard, both

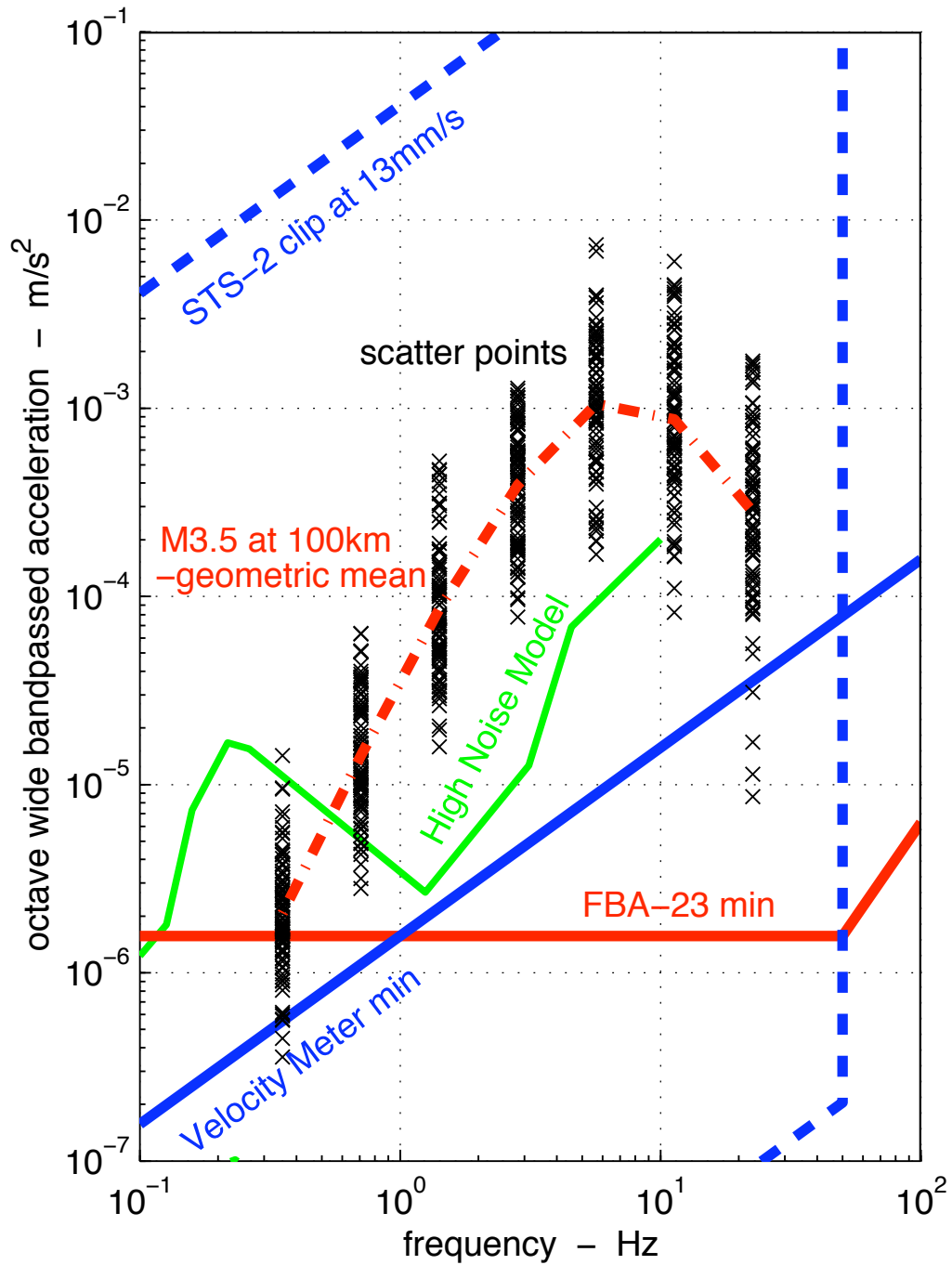


Figure 2.9: Data scatter and geometric mean for M3.5 at 100km. The crosses are the individual data points from each timeseries (as in Figure 2.7), and their geometric mean is represented by the thick dashed-dotted line. Instrument and noise lines are similar to Figure 2.6.

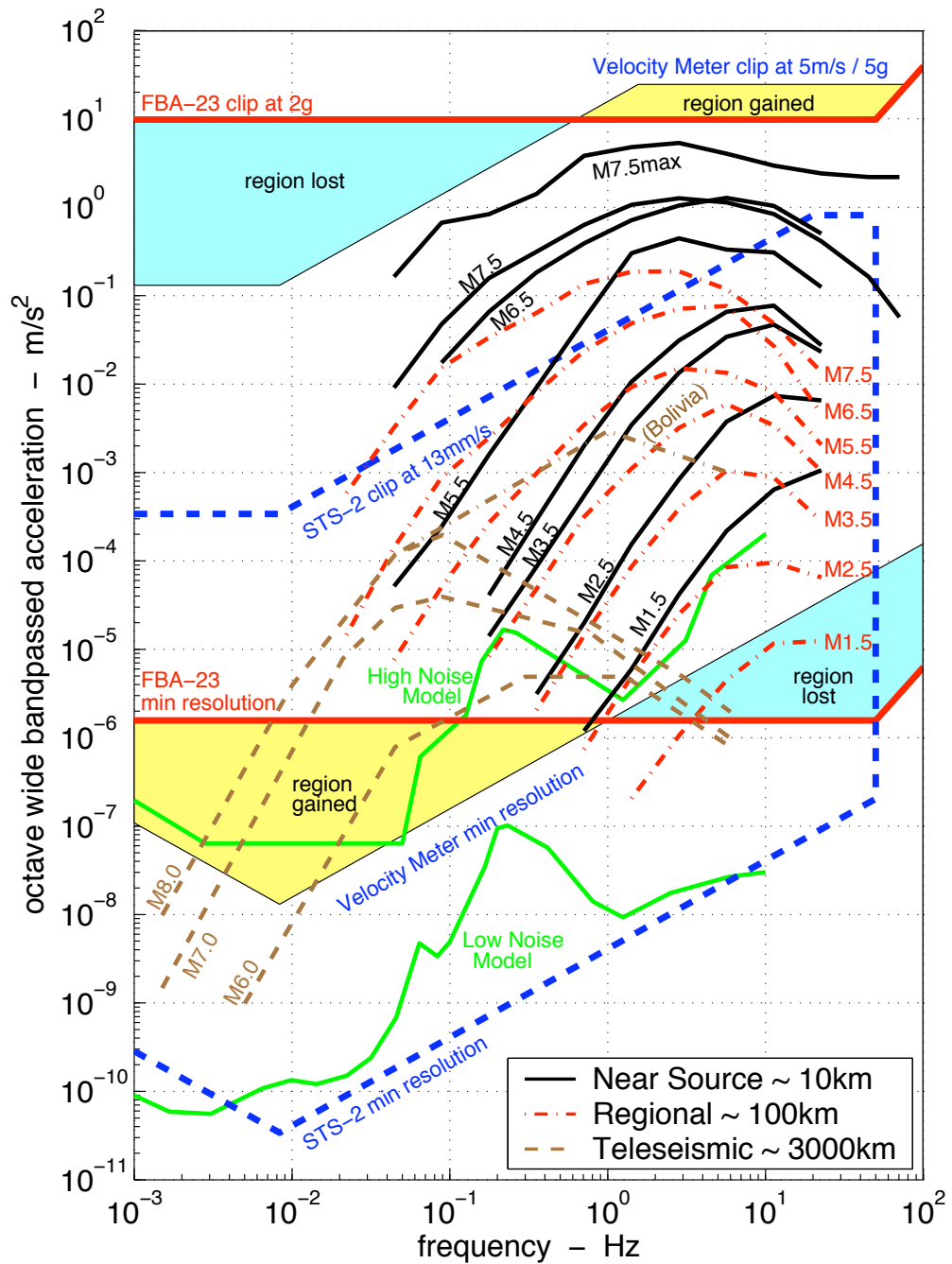


Figure 2.10: Frequency - amplitude plot — showing advantages of recording strong motion velocity. As Fig 2.1, with on-scale motions recorded by the hypothetical low-gain broadband seismometer lying between the solid blue lines. The areas shaded light blue are regions of frequency-amplitude space that are recorded by the FBA-23, but not recorded by the hypothetical low-gain broadband seismometer. Areas shaded yellow are regions of frequency-amplitude space that are recorded by the hypothetical low-gain broadband seismometer, but not recorded by the FBA-23. (see text for further explanation)

instruments would be equally effective in recording the strong motion data gathered to date.

The yellow shading in Figure 2.10 indicates regions of frequency-amplitude space that can be recorded by the hypothetical instrument, but are not presently recorded by the accelerometer. For the same dynamic range, the low-gain velocity instrument would record a larger range of Earth signals at periods greater than $1Hz$ than the accelerometer. The potential of this hypothetical device for measuring long-period motions from basin amplifications of small, local earthquakes is obvious. Teleseismic energy at longer periods, as well as energy from smaller events at teleseismic distances, would also be recorded. Regions of frequency-amplitude space presently recorded by the accelerometer, but not recorded by the hypothetical instrument, are indicated by the blue shading in Figure 2.10.

Note that the lines of geometric mean are not representative for some large, deep teleseismic events. The teleseismic database includes the M8.2 9 June 1994 637km deep focus Bolivia event, and the median line for data from this event alone is also plotted on Figure 2.10. Records from this earthquake contain interesting high frequency energy not present at teleseismic distances during shallower events.

2.5.3 Recovery of Acceleration

High frequency acceleration signals derived from a single differentiation of an STS-2 velocity timeseries are examined to demonstrate the likelihood of good recovery of acceleration data from the hypothetical instrument. Figure 2.11 presents a comparison of acceleration records from an STS-2 and an FBA-23. The record in question, from a M4.5 Northridge aftershock on 27 January 1994, recorded by the nearby SCSN station at Calabasas (CALB), had a recorded peak velocity (STS-2) of $1.24cm/s$, within 95% of clipping the instrument. There is a close correlation of these signals, even near the clipping limit of the STS-2. A similar capability to recover ground acceleration from the hypothetical instrument is anticipated.

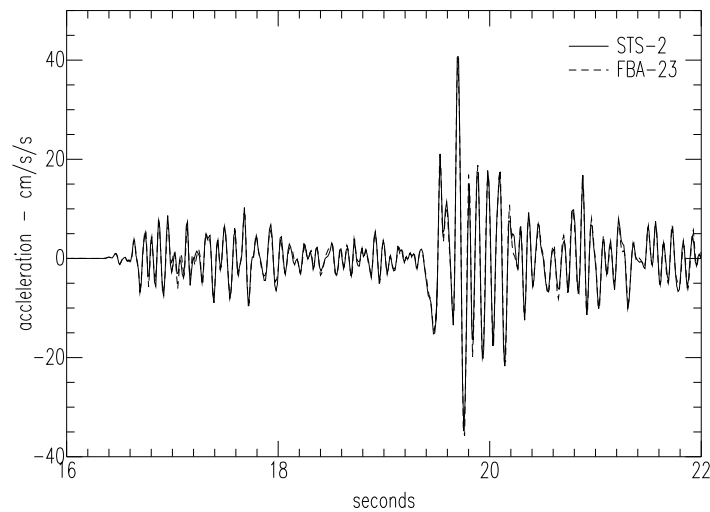


Figure 2.11: Comparison of acceleration records from a differentiated STS-2 (solid line) and an FBA-23 (dashed line). The records are from a M4.5 Northridge aftershock on 27 January 1994 recorded at Calabasas, CALB, N-S Component, 12km from the epicenter. Timeseries are from 80sps channels, with a low-pass filter at 20Hz.

2.6 ‘Strong Motion’ Recordings at Teleseismic Distances

The global seismic network and database IRIS-GSN (www.iris.washington.edu) has 1sps accelerometer channels (mainly FBA-23’s) at many stations to record long-period data from the largest earthquakes. These events may cause motions that may over-drive the current broadband seismometers, even at teleseismic distances. Figures 2.12, 2.13 and 2.14 show an example of long-period motions recorded by this channel. The recordings are from station SNZO in New Zealand, and are from the M8.1 25 March 1998 event located near Balleny Island, at a distance of 2900km. The instruments at the station are a Geotech KS-36000-i down-hole seismometer (similar to the STS-2) and an FBA-23. This record is within 15% of clipping a $\pm 13\text{cm/s}$ STS-2 — the earthquake actually clipped a Guralp CMG-3T (station SBA) and a Geotech/Teledyne KS-54000 (station VNDA) both set to about $\pm 9\text{mm/s}$ and both at a distance of 1700km from the epicenter in Antarctica. It is clear from the records that the FBA-23 is capable of recording the event well out to periods up to about 50 seconds. This clearly shows the usefulness of the strong motion instrument

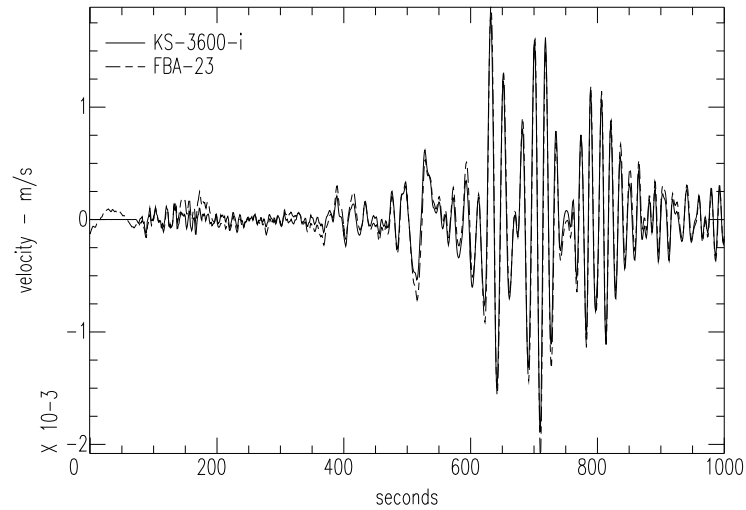


Figure 2.12: Velocity time series of 1 sps integrated FBA-23 (dashed line - high-pass filter at 300 s) and the 20 sps KS-3600-i (solid line - decimated to 1 sps) recording of the Z-component of the M8.1 Balleny Island earthquake from IRIS-GSN Station SNZO at 2900 km .

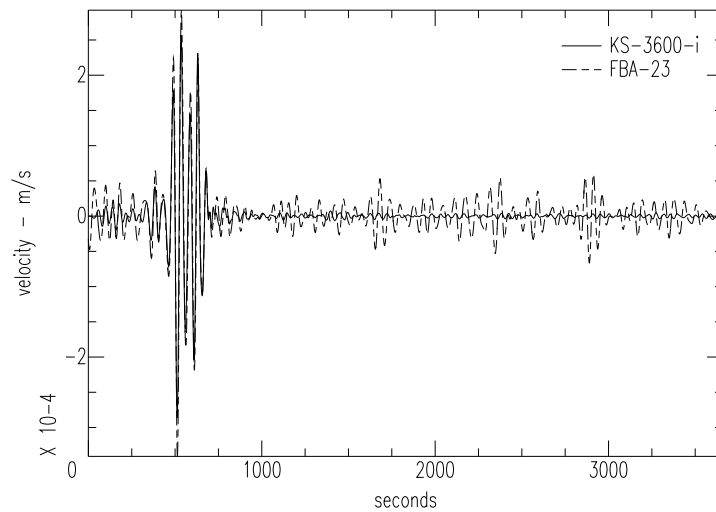


Figure 2.13: As Figure 2.12, but with a bandpass from 37.5 to 75 seconds, clearly showing the FBA-23 recording (dashed line) is capable of recovering long-period motion up to 50 seconds.

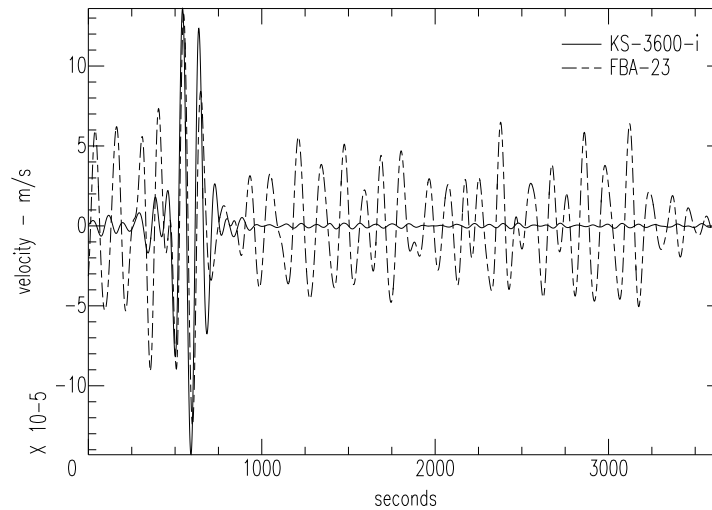


Figure 2.14: As Figure 2.12, but with a bandpass from 75 to 150 seconds, showing the FBA-23 recording (dashed line) is not easily resolved above the instrument noise at these amplifications.

at the IRIS-GSN stations, especially in the event of a great M9 earthquake, which could clip the high-gain broadband instruments for great distances. A low-gain velocity recording device would be ideally suited to deployment in future IRIS-GSN stations, as well as in the proposed Advanced National Seismic System.

2.7 Summary

Although the existing strong motion accelerometers generally perform well, several undesirable features of their response could be remedied by utilizing a strong motion sensor with a better long-period response.

Two main issues are addressed. The first issue is that records from accelerographs must be integrated twice to recover ground displacement. This double integration is an unstable procedure. In order to achieve reasonable displacements we often need to apply numerous adhoc assumptions. The second issue is that the accelerations from long-period signals (periods longer than 10 seconds) are very small. Even with $140dB$ of dynamic range, the signal-to-noise ratio of accelerometer records is poor for distant earthquakes. Potentially

valuable basin effects from small local earthquakes are also not recorded by the current accelerometers.

It is shown that both these problems would be alleviated by employing the hypothetical strong motion velocity instrument described here. This instrument would better utilize the large dynamic ranges — currently up to 7 orders of magnitude — available to the instrument designer by virtue of modern 24-bit digitisers.

The seismological community would benefit from this richer range of recorded motion, as many current networks built and maintained (in mostly urban areas) by the earthquake engineering community include only strong motion accelerometers. With the deployment of an instrument of the type discussed here, a station would record increased long-period data from near-source events of small magnitudes, medium-sized regional events and larger teleseisms. Continuous telemetry from a dense network of these strong motion stations would also aid development and the eventual reliability of a future real-time earthquake early warning system.

Using the proposed instrument, the engineering community would have access to reliable estimates of near-source ground displacements without compromising the quality of acceleration records. Improved measurements of the near-source displacement records would be of important use for the development of future structural design codes, though as will be illustrated in subsequent Chapters, permanent displacements are as difficult to recover with this instruments as they are from accelerometers. Further, the strong motion velocity meter is equally sensitive to tilt as any other inertial sensor.

A strong motion velocity seismometer would essentially be a low-gain version of existing broadband seismometers, such as the Weilandt-Streckeisen STS-2. Thus its cost would also be similar to other broadband seismometers, which at current prices is many times more than current $140dB$ accelerometers. Unfortunately, so would its size and weight. Thus the clear advantages are likely to be offset by significantly greater cost, size and weight than an accelerometer, which would make it unwieldy for dense building instrumentation.